◆ Human Brain Mapping 37:2305–2318 (2016) ◆

Differential Involvement of Brainstem Noradrenergic and Midbrain Dopaminergic Nuclei in Cognitive Control

Stefanie Köhler, Karl-Jürgen Bär,* and Gerd Wagner

Department of Psychiatry and Psychotherapy, Psychiatric Brain and Body Research Group Jena, University Hospital Jena, 07743, Germany

Abstract: Several lines of evidence suggest that the lateral prefrontal cortex (PFC), the dorsal anterior cingulate cortex (dACC), the parietal cortex, and the thalamus are central cortical nodes in a network underlying cognitive control. However, the role of catecholamine producing midbrain and brainstem structures has rarely been addressed by functional magnetic resonance imaging (fMRI). We hypothesized differential activation patterns in the ventral tegmental area (VTA)/substantia nigra (SN) and locus coeruleus (LC) with respect to the degree of cognitive control during a Stroop task in healthy subjects. Forty-five healthy subjects were investigated by the manual version of the Stroop task in an event-related fMRI design. We observed significant BOLD activation of both the SN/VTA and LC during the Stroop interference condition (incongruent vs. congruent condition). LC, but not SN/VTA activation significantly correlated with the Stroop interference. Interestingly, a significant linear decrease in BOLD activation during the incongruent condition during the experiment was mainly observed in the fronto-cingulo-striatal network, but not in SN/VTA and LC. Using psychophysiological (PPI) analyses, a significant functional connectivity during cognitive control was observed between SN/VTA and the nigrostriatal/mesolimbic dopaminergic system. For the LC, distinct functional connectivity pattern was observed mainly to the dorsolateral and ventrolateral PFC. Both regions revealed significant functional connectivity to the dACC, parietal and occipital regions. Thus, we demonstrate for the first time that functional activation patterns in the SN/VTA and the LC are modulated by different demands of cognitive control. In addition, these nuclei exhibit distinguishable functional connectivity patterns to cortical brain networks. *Hum Brain Mapp 37:2305–2318, 2016.*

Key words: fMRI; cognitive control; locus coeruleus; ventral tegmental area; functional connectivity

Additional Supporting Information may be found in the online version of this article.

Contract grant sponsor: German Research Foundation; Contract grant number: DFG WA 3001/3-1.

Financial disclosures: All authors report no biomedical financial interests or potential conflicts of interest.

*Correspondence to: K.-J. Bär, Department of Psychiatry and Psychotherapy, University Hospital, Philosophenweg 3, 07743 Jena, Germany. E-mail: Karl-Juergen.Baer@med.uni-jena.de

Received for publication 11 September 2015; Revised 23 February 2016; Accepted 24 February 2016.

DOI: 10.1002/hbm.23173

Published online 11 March 2016 in Wiley Online Library (wileyonlinelibrary.com).

INTRODUCTION

The term "cognitive control" relates to a number of operations that enable the cognitive system to successfully pursue specific cognitive tasks, such as maintaining and manipulating goal-related information or inhibiting and overriding prepotent responses [Botvinick et al., 2001]. On the neural level, cognitive control is characterized by a dynamic interplay between prefrontal, posterior parietal and subcortical structures [Miller and Cohen, 2001]. The lateral prefrontal cortex (PFC), consisting of the dorsolateral and ventrolateral prefrontal cortex (DLPFC, VLPFC), the dorsal anterior cingulate cortex (dACC), the parietal cortex and the thalamus, are regarded as central nodes of this cognitive control network [Mansouri et al., 2009].

Dopamine-producing (DA) neurons are mainly located in the ventral tegmental area (VTA) and substantia nigra (SN) and are part of two proposed systems: the nigrostriatal and the mesolimbic dopaminergic system [Ungerstedt, 1971]. The nigrostriatal system originates from the SN and projects to thalamic nuclei, the caudate nucleus, and the putamen. The dorsal striatum receives strong input from the prefrontal as well as from premotor and posterior parietal brain regions [Haber et al., 2000; Parent, 1990]. This system is mainly associated with cognitive functions and motor outcomes [Alexander et al., 1986], in particular with cognitive flexibility and the development of stimulus-response (S-R) contingencies. The mesolimbic dopaminergic system arises from the VTA and the medial part of the SN. It has dense projections to the nucleus accumbens (NAc), but also to other limbic regions including the hippocampus, amygdala, and the medial PFC [Ikemoto, 2007]. The system contributes to reward-guided behavior and motivation. Haber [2003] provided substantial evidence for the close interaction between both dopaminergic systems, reflecting the DA-dependent interaction between motivational and cognitive processes. In addition, studies investigating cognitive control processes in subjects with abnormal DA transmission consistently reported an altered regional cerebral blood flow (rCBF) or BOLD activation in the fronto-cingulate network during the Stroop task [Bolla et al., 2004; Salo et al., 2009].

The locus coeruleus (LC) is a brainstem structure containing noradrenaline-producing neurons. Axon terminals of LC neurons are distributed throughout most cortical and subcortical areas. The frontal lobe and the cingulate cortex have been shown to contain the highest density of noradrenergic (NA) fibers of all neocortical areas [Fuxe et al., 1968], which enable the modulation of cognitive flexibility and executive functioning of this brain network [Foote et al., 1983; Sara and Bouret, 2012]. In their review, Aston-Jones and Cohen [2005] emphasize the specific role of the LC in cognitive flexibility. The authors propose that enhanced LC activity produces a temporally specific release of noradrenaline, which increases the gain of specific task-associated cortical networks and optimizes task-appropriate behavior. Several studies in rats provided evidence for the important involvement of LC in cognitive flexibility [Devauges and Sara, 1990]. It was reported that attentional set shifting is mainly dependent on the NA system influencing the medial PFC, which corresponds to the ACC in humans [Tait et al., 2007]. Reducing LC activity in rats by a centrally acting alpha 2-adrenergic agonist clonidine negatively affects response time and accuracy in attentional and memory tasks [Mair et al., 2005].

The so-called "network reset" theory by Bouret and Sara [2005] suggests that the activation of the LC-NA system in response to a particular sensory event will produce or facilitate the dynamic reorganization of neural networks leading to new functional networks that regulate the adaptive behavioral output. Corbetta et al. [2008] has linked in more detail the LC-NA system to attention shifting and cognitive flexibility. The authors described two separate functional anatomical networks underlying attentional processing. First, the dorsal fronto-parietal network that contains the DLPFC and the dorsal parietal cortex as core regions. It is involved in directing attention and top-down modulation of expected stimuli as well as generating appropriate stimulus-response contingencies. Second, the ventral fronto-parietal network mainly consisting of the temporo-parietal junction, VLPFC and anterior insula, is responsible for the detection of behaviorally salient stimuli [Corbetta et al., 2008]. Depending on the incoming stimuli, signals from the LC influence adaptive state shifts between the ventral and dorsal fronto-parietal networks. Thus, changes in the activation pattern of the LC during transition from an exploratory to a task-focused state are accompanied by a deactivation of ventral and an activation of dorsal networks [Corbetta et al., 2008].

However, the role of LC in cognitive tasks has rarely been investigated in humans by means of functional neuroimaging. Coull et al. [1999] demonstrated that clonidine increases the effective connectivity from LC to parietal cortex during an attentional task using positron emission tomography scanning. Raizada and Poldrack [2008] observed a complexity-dependent covariation of the LC and VLPFC in an audiovisual task with unpredictably varying stimulus onset asynchrony [SOA], supporting the theory of Corbetta et al. [2008].

Thus, there is strong evidence for the notion that NA and DA produced in brainstem/midbrain nuclei are crucially involved in cognitive control processes by exerting a modulatory influence on fronto-cingulo-striatal and fronto-cingulo-parietal networks. However, according to our knowledge the activation dynamics as well as the task-dependent functional connectivity of these nuclei during a cognitive control task have not yet been investigated using functional magnetic resonance imaging (fMRI). Therefore, the main goal of this study was to elucidate functional activation patterns and functional connectivity of noradrenaline and DA producing areas as well as the dynamics of the BOLD activation changes during the Stroop Color-Word task [Stroop, 1935]. It is a well-established

experimental paradigm to measure cognitive and especially inhibitory control, which requires an inhibition of an overlearned, prepotent response tendency (reading the word), in favor of an unusual, less prepotent action (reading the ink). We assumed a significant functional connectivity of the DA nuclei with the fronto-cingulo-striatal network, which enhances its strength with increasing cognitive control. Based on the theory of Corbetta et al. [2008], we expect changes in the functional connectivity of the LC with the dorsal fronto-cingulo-parietal network during an increased demand of cognitive control.

MATERIALS AND METHODS

Subjects

Forty-seven subjects (age $M = 27.7$ years; SD = 7.7 years; range: 18–56 years; 28 females) participated in this study. They were recruited from the local community. Subjects with past or current neurological or psychiatric diseases according to M.I.N.I [Sheehan et al., 1998] and/or first-degree relatives with Axis I psychiatric disorders were excluded from the study. None of the study participants was taking any psychopharmacological medication.

Two subjects were excluded from the final analysis due to movement artifacts exceeding 3 mm or 3° rotation. Thus, 45 subjects were finally analyzed (age $M = 27.5$ years; SD = 7.8 years; range: 18–56 years; 26 females). All participants were German native speakers, right-handed according to the modified version of Annetts handedness inventory [Briggs and Nebes, 1975] and provided written informed consent prior to participating in the study. The study protocol was approved by the Ethics Committee of the University of Jena. All subjects were paid 8 Euro per hour for their participation.

Experimental Paradigm

The manual version of the Stroop Color-Word task was described in detail previously [Wagner et al., 2015]. In brief, the Stroop task consists of two conditions: a congruent and an incongruent condition. In the congruent condition, 18 color words are presented in the color denoted by the corresponding word; in the incongruent condition, 18 color words are displayed in one of three colors, which are not denoted by the word. This target stimulus was presented in the center of the display screen. Two possible answers (color words in black type) were presented in the lower visual field to minimize contextual memory demands. All subjects had to indicate as fast as possible the type of color by pressing one of two buttons (with right index or middle finger), which corresponded spatially to both possible answers. Correct answers were counterbalanced on the right and left sides of the display. Stimulus presentation time was 1500 ms with an interstimulus interval of 10.5 s. Additionally, a temporal jitter was introduced to enhance the temporal resolution. The presentation of stimuli was varied relative to the onset of a scan in 12 steps for 182 ms. This jitter was shifted over the repetition time three times per condition.

MRI Parameters

Functional data were collected on a 3 T Siemens TIM Trio whole body system (Siemens, Erlangen, Germany) equipped with a 12-element receive-only head matrix coil. Head immobilization was done using head pads within the head coil. T_2*-weighted images were obtained using a gradient-echo EPI sequence (TR = 2700 ms, TE = 30 ms, flip angle = 90°) with 48 contiguous transverse slices of 2.7 mm thickness and an interslice gap of 10% covering the entire brain and including the lower brainstem. Matrix size was 72 × 72 pixels with in-plane resolution of 2.67 × 2.67 mm^2. A series of 220 whole-brain volume sets were acquired in one session. High-resolution anatomical T1-weighted volume scans (MP-RAGE) were obtained in sagittal orientation (TR = 2300 ms, TE = 3.03 ms, TI = 900 ms, flip angle = 9°, FOV = 256 mm, matrix = 256 × 256 mm^2, number of sagittal slices = 192, acceleration factor (PAT) = 2, TA = 5:21 min) with an isotropic resolution of 1 × 1 × 1 mm^3.

Univariate Functional Data Analyses

For image processing and statistical analyses, we used the SPM8 software (http://www.fil.ion.ucl.ac.uk/spm). Data preprocessing and single-subject level analyses were identical to our previous studies [Wagner et al., 2015]. The first four images were discarded to obtain steady-state tissue magnetization. The remaining 216 images were corrected for differences in time acquisition by sinc interpolation, realigned at the first image. The coregistered anatomical images were segmented using the tissue probability maps of the ICBM template in SPM8. Functional images were then spatially normalised to the MNI space using spatial normalisation parameters estimated during the segmentation process. The whole-brain data were smoothed with a Gaussian filter of 6 mm FWHM and were high-pass filtered with a cutoff period of 128 s and corrected for serial correlations choosing AR(1).

Subsequently, data were analyzed voxelwise within the general linear model to calculate statistical parametric maps of t statistics for condition-specific effects. Individual movement parameters entered a fixed effects model at a single-subject level as covariates of no interest. A fixed-effects model at a single-subject level was performed to create images of parameter estimates, which were then entered into a second-level analysis. For the second level group comparison, we set up an ANOVA design with a within-subjects factor TASK (congruent and incongruent condition) and tested for the interference contrast incongruent vs. congruent condition. For the whole-brain

analyses, the statistical comparisons were thresholded on the voxel-level at $P < 0.001$ (uncorrected) and $P < 0.05$ FWE corrected at the cluster-level as recently recommended by Woo et al. [2014].

Due to the small size of brainstem nuclei and therefore smaller expected number of activated contiguous voxels, we additionally performed an ROI analysis in the brainstem using a mask image, which was created by means of the WFU PickAtlas (http://fmri.wfubmc.edu/software/PickAtlas) and comprised the midbrain and the upper brainstem. The statistical comparisons were thresholded on the voxel-level at $P < 0.001$ (uncorrected) and on a more liberal cluster-extent threshold, which corresponded to the number of expected voxels per cluster k_e.

fMRI Analysis of Brainstem/Cerebellum Using SUIT Toolbox

To improve the normalization procedure and to verify statistical results in the brainstem detected at the whole-brain level and in the ROI analysis, data were normalized to the spatially unbiased infra-tentorial template (SUIT, version 3.1) [Diedrichsen, 2006]. The SUIT toolbox provides a new high-resolution atlas template of the human brainstem and cerebellum, based on the anatomy of 20 young healthy individuals. Using the SUIT toolbox, we applied the following preprocessing steps: (i) segmentation of the whole-brain image, (ii) cropping of the image, retaining only the cerebellum and brainstem, (iii) normalization using the DARTEL engine [Ashburner, 2007] that uses gray and white matter segmentation maps produced during cerebellar isolation to generate a flowfield using Large Deformation Diffeomorphic Metric Mapping [Beg et al., 2005], (iv) reslicing to a voxel size of $2 \times 2 \times 2$ mm^3, and (v) smoothing with Gaussian filter of 4 mm FWHM. After high-pass filtering (128 s) and correction for serial correlations [AR(1)], a fixed-effects model (the same as at the whole-brain level) at the single-subject level was set-up with preprocessed functional brainstem/cerebellum images to create images of parameter estimates for the subsequent random-effects group analyses (RFX). The statistical comparisons at the brainstem/cerebellum level were thresholded on the voxel-level at $P < 0.001$ (uncorrected) and corrected at the cluster-level according to the expected voxels per cluster.

Correlational Analysis

The significance of a relationship between Stroop interference score (response time difference between incongruent and congruent conditions) and neural activation during the incongruent vs. congruent condition contrast were investigated using the regression analysis. The statistical comparisons were thresholded on the voxel-level at $P < 0.001$ (uncorrected) and $P < 0.05$ FWE corrected at the cluster-level. Statistical comparisons based on the ROI analysis in the brainstem were thresholded on the voxel-level at $P < 0.001$ (uncorrected) and on a more liberal cluster-extent threshold, which corresponded to the number of expected voxels per cluster k_e. For this purpose, we used the mask image of the brainstem, which was created by means of the WFU PickAtlas.

We further performed a regression analysis with the Stroop interference score using the images of parameter estimates (incongruent vs. congruent conditions) from the brainstem/cerebellum analysis as preprocessed with the SUIT toolbox in order to confer the results of the whole-brain analysis. The statistical comparisons on the brainstem level were thresholded on the voxel-level at $P < 0.001$ (uncorrected) and on the cluster-level according to the expected voxels per cluster.

Practice-Related Signal Changes in Neuronal Activation

To examine the signal course across time, we conducted a parametric modulation analysis, which modulates the amplitude of the predicted HRF. Based on the behavioral data, we modeled the linear signal decrease as a covariate of interest to investigate whether, and in which regions, the change in BOLD response in the incongruent Stroop condition followed the anticipated linear time course. In addition, we modeled the linear signal increase as a covariate of interest to test for potential signal increases. Voxel-by-voxel t-tests were individually computed for each subject on the first level. The contrast images derived from these analyses were then entered into the group-level one-sample t-tests, which were thresholded on the voxel-level at $P < 0.001$ (uncorrected) and FWE corrected at the cluster-level. Lowering the cluster-level threshold to a more liberal cluster-extent threshold, we tested for linear signal changes in the brainstem based on the ROI analysis as described above. We further examined the linear BOLD signal changes in the incongruent Stroop condition in the brainstem/cerebellum only, as preprocessed with the SUIT toolbox and applied a statistical threshold of $P < 0.001$ (uncorrected) on the voxel-level at and on the cluster-level according to the expected voxels per cluster.

Psychophysiological Interactions (PPI)

Based on our initial hypothesis and the results of the significant univariate analysis (incongruent vs. congruent contrast), a PPI analysis as implemented in SPM8 was used to further elucidate changes in the functional connectivity between the dopaminergic SN/VTA as well as the NA LC and the neural network during cognitive control. First, we created a mask image from the cluster of significant BOLD activation difference between the incongruent and congruent condition comprising the SN/VTA as well as LC. Then, the individual local maximum within this mask image was determined to build the individual ROI

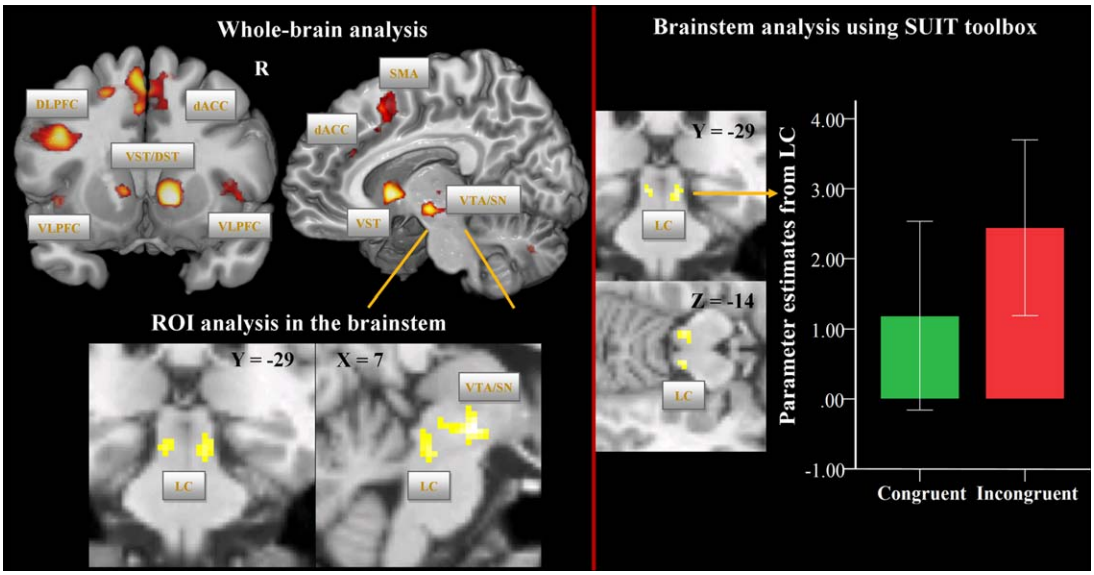

Figure 1.

Univariate fMRI analysis: incongruent vs. congruent Stroop task condition. On the upper left side, brain regions are depicted, which show increased BOLD signal during the incongruent vs. congruent condition at the whole-brain level (voxel-level: $P < 0.001$ uncorr., cluster-level: $P < 0.05$, FWE corr.). On the lower left side, BOLD activation differences (voxel-level: $P < 0.001$ uncorr., cluster-level: according to the number of expected voxels per cluster k_e) are illustrated based on the ROI analysis in the brainstem. The mask image was created using the WFU PickAtlas and comprised the midbrain and the upper brainstem. On the right side, brain regions are depicted, which show increased BOLD signal during the incongruent vs. congruent conditions at the level of the brainstem/cerebellum as preprocessed with the SUIT toolbox and using 4 mm FWHM smoothing (voxel-level: $P < 0.001$ uncorr., cluster-level: according to the number of expected voxels per cluster k_e). The box plot shows the parameter estimates for the congruent and incongruent conditions as extracted from the LC cluster. Abbreviations: DLPFC, dorsolateral prefrontal cortex; VLPFC, ventrolateral prefrontal cortex; dACC, dorsal anterior cingulate cortex; SMA, supplementary motor area; VST, ventral striatum; DST, dorsal striatum; VTA/SN, ventral tegmental area/substantia nigra; LC, locus coeruleus.

of 3 mm radius sphere. In two subjects, we were not able to create an LC-ROI and to extract the time series. The averaged time series extracted from these ROIs from the contrast incongruent vs. baseline was adjusted for the effects of interest. An individual design matrix was created, with one regressor representing the activation time course in the SN/VTA and LC respectively, one regressor representing the time dependent change as a psychological variable of interest (incongruent vs. congruent Stroop condition from the design matrix), and a third regressor representing the element-by-element product of the previous two (the PPI term). The PPI analysis was individually computed for each subject and the contrast images derived from these analyses were then entered into the group-level one-sample t-test, which was thresholded on the voxel-level at $P < 0.001$ (uncorrected) and $P < 0.05$ FWE corrected at the cluster-level.

Behavioral Data Analysis

The behavioral analyses were performed by means of SPSS Statistics V22. Using the paired t-test the difference in the response times between the incongruent and congruent Stroop conditions were tested for significance. Furthermore, potential differences in the response accuracy were analyzed using the Wilcoxon signed-rank test. Practice-related changes in response times were examined by means of linear regression analysis.

RESULTS

Behavioral Performance

Subjects responded significantly faster [$t(44) = 6.22$; $P < 0.001$] in the congruent than in the incongruent condition of the Stroop task, indicating a reliable induction of the Stroop interference effect [Stroop, 1935]. The averaged Stroop interference time, defined as difference in reaction time between incongruent and congruent condition, was $M = 250.82$ ms (SD = 270.6). In both conditions, high levels of accuracy were obtained: in the congruent condition 97.4% (SD = 1.53), and in the incongruent condition 92.3% (SD = 1.71). The nonparametric Wilcoxon test revealed a significant accuracy difference between congruent and

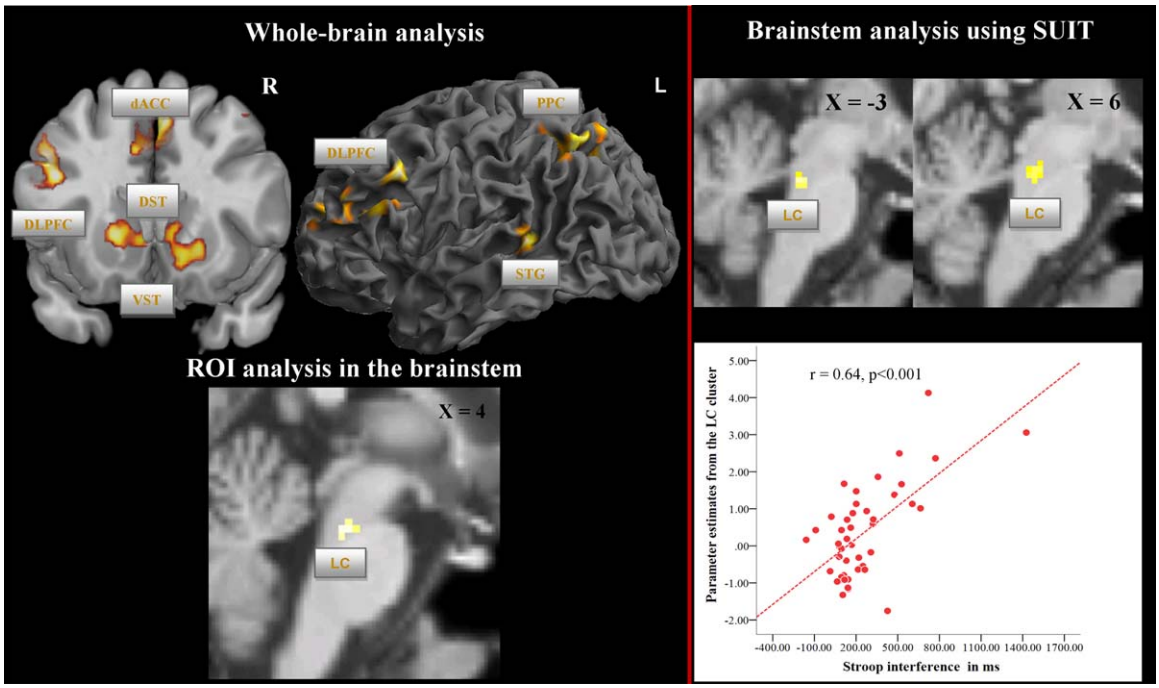

Figure 2.

Univariate fMRI analysis: correlation between Stroop interference time and BOLD activation in the contrast incongruent vs. congruent condition. On the upper left side, significant correlation between Stroop interference time (difference in response time between incongruent and congruent condition) and BOLD activation in the contrast incongruent vs. congruent condition is presented at the whole-brain level (voxel-level: $P < 0.001$ uncorr., cluster-level: $P < 0.05$, FWE corr.). On the lower left side, significant correlation between Stroop interference time and BOLD activation is presented based on the ROI analysis in the brainstem (voxel-level: $P < 0.001$ uncorr., cluster-level: according to the number of expected voxels per cluster k_e). On the upper right side, significant correlation between Stroop interference time and BOLD activation is presented at the level of the brainstem/cerebellum as preprocessed with the SUIT toolbox and using 4 mm FWHM smoothing (voxel-level $P < 0.001$: uncorr., cluster-level: according to the number of expected voxels per cluster k_e). In the right lower corner, the scatterplot of the significant positive correlation between parameter estimates from the LC cluster and Stroop interference time is depicted. Abbreviations: DLPFC, dorsolateral prefrontal cortex; dACC, dorsal anterior cingulate cortex; VST, ventral striatum; DST, dorsal striatum; STG, superior temporal gyrus; PPC, posterior parietal cortex; LC, locus coeruleus.

incongruent condition ($Z = -3.51$, $P = <0.001$). The linear regression analysis revealed a significant linear decrease in RT in the whole group in the incongruent condition ($R^2 = 0.85$, $P < 0.001$).

Univariate fMRI Analyses

Incongruent vs. congruent Stroop conditions

Comparing the incongruent with the congruent condition, we detected increased, mainly left lateralized, BOLD activations especially in the VLPFC, DLPFC, dACC, SMA, mediodorsal thalamus, insula, the ventromedial head of the caudate, the NAc, and putamen as well as cerebellum (Fig. 1, Supporting Information Table S1). Similarly, the medial part of the midbrain comprising VTA and the medial portion of the SN showed increased BOLD activation patterns during incongruent vs. congruent condition (voxel-level: $P < 0.001$ uncorr.; cluster-level: $P < 0.05$, FWE corrected, Fig. 1, left half).

As shown in Figure 1, based on the ROI analysis in the brainstem and using a more liberal cluster-extent threshold, which corresponded to the number of expected voxels per cluster $k_{e,}$ we additionally detected a significant activation difference (voxel-level: $P < 0.001$ uncorr.) in two clusters in the brainstem, which most likely correspond to the left ($x = -4$, $y = -26$, $z = -16$, $t = 3.84$, $P < 0.001$, cluster size = 37) and right LC ($x = 8$, $y = -28$, $z = -16$, $t = 3.98$, $P < 0.001$, cluster size = 17), as identified from the known anatomical localization [Naidich et al., 2009; Nieuwenhuys, 1985].

Brainstem/cerebellum analysis using SUIT toolbox: Incongruent vs. congruent Stroop conditions

Applying more sophisticated brainstem/cerebellum normalization and a smoothing filter of 4 mm FWHM, we

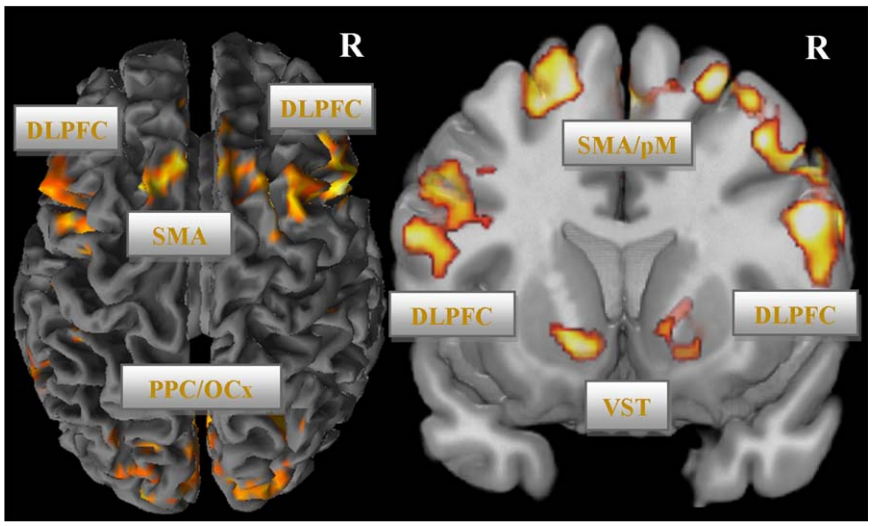

Figure 3.
Practice-related BOLD signal decrease in the incongruent condition (voxel-level: $P < 0.001$ uncorr., cluster-level: $P < 0.05$, FWE corr.). Abbreviations: DLPFC, dorsolateral prefrontal cortex; dACC, dorsal anterior cingulate cortex; SMA, supplementary motor area; VST, ventral striatum; PPC, posterior parietal cortex; OCx, occipital cortex.

could confer the results of the whole-brain and ROI analyses. As illustrated in the Figure 1 (right half) and in the Supporting Information Figure S1 (unsmoothed data), we observed in the incongruent in contrast to congruent Stroop condition significantly increased BOLD signal in the left ($x = -6$, $y = -28$, $z = -13$, $t = 4.01$, $P < 0.001$, cluster size = 26) and right LC ($x = 8$, $y = -28$, $z = -15$, $t = 4.14$, $P < 0.001$, cluster size = 16).

Additionally, significantly increased BOLD activation in the incongruent vs. congruent condition was detected in the clusters comprising VTA/SN ($x = 8$, $y = -18$, $z = -8$, $t = 3.83$, $P < 0.001$; cluster size = 40) as well as in the right ($x = 12$, $y = -70$, $z = -35$, $t = 4.69$, $P < 0.001$; cluster size = 99) and left cerebellum ($x = -14$, $y = -44$, $z = -29$, $t = 4.62$, $P < 0.001$; cluster size = 21).

Correlational analysis

As illustrated in Figure 2 (left half) and Supporting Information Table S2, a positive correlation between the

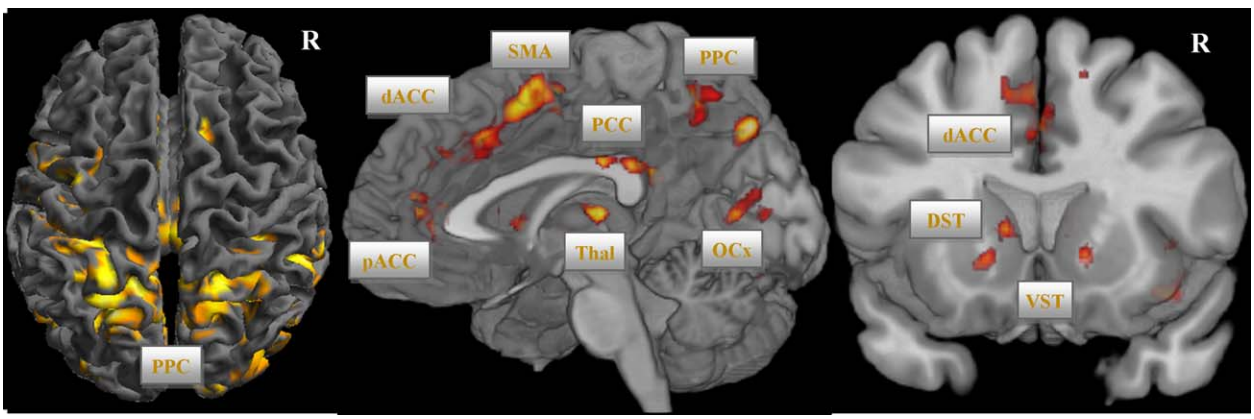

Figure 4.
PPI analysis using VTA/SN as seed region (voxel-level $P < 0.001$ uncorr., cluster-level, $P < 0.05$, FWE corr.). Abbreviations: DLPFC, dorsolateral prefrontal cortex; dACC, dorsal anterior cingulate cortex; SMA, supplementary motor area; VST, ventral striatum; PCC, posterior cingulate cortex; PPC, posterior parietal cortex; OCx, occipital cortex

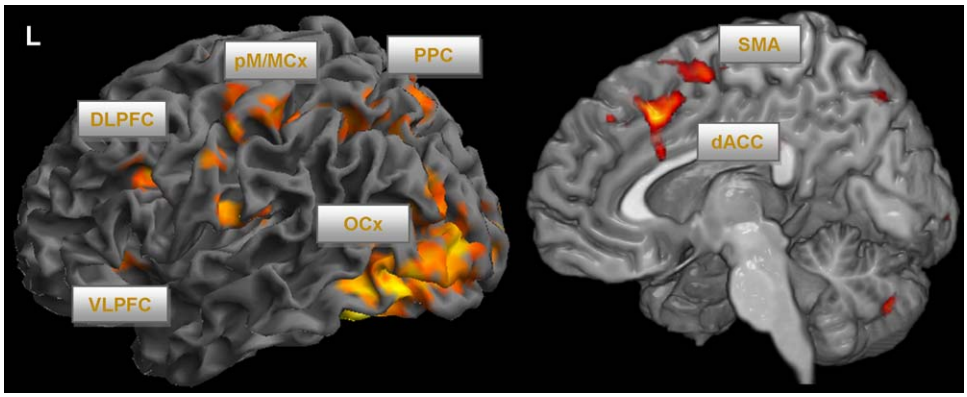

Figure 5.
PPI analysis using LC as seed region (voxel-level: $P < 0.001$ uncorr., cluster-level: $P < 0.05$, FWE corr.). Abbreviations: DLPFC, dorsolateral prefrontal cortex; VLPFC, ventrolateral prefrontal cortex; dACC, dorsal anterior cingulate cortex; SMA, supplementary motor area; pM/MCx, premotor/motor cortex; PPC, posterior parietal cortex; OCx, occipital cortex

RT interference scores and BOLD activation during the Stroop interference contrast (whole-brain analysis, incongruent vs. congruent condition; $P < 0.001$; cluster-level FWE corrected) was observed bilaterally in the DLPFC, bilaterally in the putamen and caudate, NAc, as well as in dACC extending to the SMA, in the left superior temporal gyrus (STG) and precuneus. Importantly, in the ROI analysis, a significant positive correlation (Fig. 2) was also found in the brainstem, presumably most likely corresponding to LC ($x = -2$, $y = -30$, $z = -26$, $t = 3.95$, $P < 0.001$; cluster size = 17), but not in the SN/VTA. The LC position was slightly different along the rostrocaudal axis in comparison to the contrast incongruent vs. congruent condition.

Brainstem/cerebellum analysis using SUIT toolbox: Correlational analysis

Using images of parameter estimates in the brainstem/cerebellum as preprocessed with the SUIT toolbox, we could confer the results of the regression analysis at the whole-brain level and based on the ROI analysis. We detected a significant positive correlation with the Stroop interference score (on the right side in Fig. 2 and Supporting Information Fig. S1) in a cluster comprising the left ($x = -2$, $y = -32$, $z = -23$, $t = 4.5$, $P < 0.001$) and right LC ($x = 6$, $y = -28$, $z = -21$, $t = 4.03$, $P < 0.001$; cluster size = 32), but not in the SN/VTA. Furthermore, a number of significant clusters were detected in the left and right cerebellum (Supporting Information Table S6).

Practice-related signal changes in neuronal activation over time

Group analysis of the linear signal decrease yielded significant results in several brain areas of the fronto-cingulo-striatal network, but not in the VTA/SN and LC in the whole-brain as well as in the ROI analyses (see Fig. 3; Supporting Information Table S3). This activation decline was mainly present in VLPFC, DLPFC, dACC extending to pre-SMA, NAc, ventromedial caudatus, putamen as well as in the left STG, inferior parietal, and occipital cortex ($P < 0.001$; cluster-level FWE corrected). No significant linear BOLD activation increases were detectable.

Brainstem/cerebellum analysis using SUIT toolbox: Practice-related signal changes in neuronal activation over time

Investigating practice-related signal changes in the brainstem/cerebellum as preprocessed with the SUIT toolbox, we could confer the results at the whole-brain level and in the ROI analysis. We did not detect any significant linear BOLD signal changes in the LC and VTA/SN. Instead, a significant linear BOLD signal decrease was detected in the left ($x = -2$, $y = -76$, $z = -21$, $t = 4.44$, $P < 0.001$; cluster size = 45) and two clusters in the right ($x = 44$, $y = -58$, $z = -27$, $t = 4.35$, $P < 0.001$; cluster size = 79), ($x = 18$, $y = -76$, $z = -25$, $t = 4.6$, $P < 0.001$; cluster size = 26) cerebellum.

PPI Analysis

Substantia nigra/ventral tegmental area

A PPI analysis was performed to reveal brain regions interacting with the SN/VTA in the Stroop interference contrast (incongruent > congruent condition). As illustrated in Figure 4 and Supporting Information Table S4, using SN/VTA as seed region, a brain network mainly including NAc, ventral caudate, putamen, thalamus, perigenual ACC, and dACC extending to SMA, insula,

superior parietal lobe, and cerebellum ($P < 0.001$; cluster-level FWE corrected) was found.

Locus coeruleus

Using LC as seed region, differences in the functional connectivity with respect to the interference contrast were primarily observed in VLPFC, DLPFC, dACC/SMA, premotor cortex, occipital cortex, in the superior parietal lobe as well as in cerebellum ($P < 0.001$; cluster-level FWE corrected), which is illustrated in Figure 5 and Supporting Information Table S5.

DISCUSSION

In this study, we demonstrate for the first time that functional activation in the midbrain (SN/VTA) and brainstem (LC) is modulated by different demands of cognitive control and that these regions show distinguishable functional connectivity patterns to specific brain networks.

Substantia Nigra/Ventral Tegmental Area

The study showed that different cognitive demands modulate the functional connectivity between the medial SN/VTA, the nigrostriatal and the mesolimbic dopaminergic systems. This pattern of connectivity is highly consistent with known neuroanatomical projections from DA neurons and recent neuroimaging studies of dopaminergic resting state functional connectivity [Tomasi and Volkow, 2014]. The DA nigrostriatal pathway conveys information to the thalamus and the dorsal striatum, and further to neurocortical regions via direct (striato-nigral) and indirect pathways [Amalric and Koob, 1993]. The mesolimbic dopaminergic system arises from the VTA and the medial part of the SN and has dense projections to the NAc, but also to other limbic regions and the medial PFC, such as the observed functional connectivity to the perigenual ACC.

The concept of cortico-striatal loops is an influential model to comprehend the functional inter-relationships between the neocortex and the striatum [Alexander et al., 1986]. In this model, the so-called "sensorimotor loop" consists of the caudal and lateral aspects of the putamen, and receives input from primary and supplementary motor areas as well as from the somatosensory cortex. The putamen projects to the globus pallidus and SN, which in turn, send projections to the thalamus. Furthermore, thalamic projections to primary and supplementary motor areas close the circuit [Alexander and Crutcher, 1990; Grahn, et al., 2008]. Another loop, the "limbic loop" encompasses the ventromedial striatum, including NAc, and the ventral caudate, which receives input from the orbital and medial PFC [Haber et al., 2000; Kunishio and Haber, 1994]. A very close match between these anatomically and functionally defined loops and present results are observable in our PPI analysis using SN/VTA as regions of interest.

Thus, it seems reasonable to conclude that the medial SN, dorsal striatum, thalamus, SMA, and dACC are mainly involved in detecting and resolving the "output" motor conflict, selecting the motor response as well as inhibiting prepotent motor responses, which arise when performing the manual version of the Stroop task. The close connection between the VTA, ventral striatum, and perigenual ACC gives rise to the assumption that the activation of this network might be additionally associated with goal-directed motivational processes, such as attributing an incentive value to selected goals [Mannella et al., 2013]. Previous research has demonstrated that the NAc is important for learning processes, which are associated with reward [O'Doherty et al., 2003, 2006]. Moreover, Tomasi and Volkow [2014] showed in an fMRI study that the temporal prediction of responses involved dopaminergic striato-cortical circuits. Interestingly, accurate responses that were rewarding per se activated the NAc stronger than inaccurate ones.

In this study, we found a linear decline of the RTs over time for the incongruent Stroop task condition. This was associated with a linear decrease in BOLD activation of the fronto-cingulo-striatal network, implying the diminished need of cognitive control over time due to adjustment. Similar results were reported in previous studies investigating practice-related effects on brain activation [Koch et al., 2006; Milham et al., 2003]. Furthermore, a linear BOLD activation decline was present in the ventral striatum, suggesting a decline in motivational processes over time. In contrast, despite this linear decline of the anatomically interconnected regions of the fronto-cingulo-striatal circuitry, no significant activation decline was observed in VTA/SN. This indicates a time invariant activation pattern and might be suggestive of an indirect influence on the brain network associated with cognitive control. The nonsignificant correlation with the Stroop interference time might add weight to this assumption.

Locus Coeruleus

The detected functional connectivity of LC during Stroop interference is in accordance with known neuroanatomical projections of NA neurons. The frontal lobe and the cingulate cortex have been shown to contain the highest density of NA fibers of all neocortical areas [Fuxe et al., 1968]. Accordingly, the PPI analysis revealed that the DLPFC and VLPFC, but also the dorsal parietal lobe, visual and motor brain areas are functionally connected with the LC activation pattern, indicating an important role of LC in cognitive conflict resolution. Further support for this notion is provided by the significant correlation between LC activation and Stroop interference time. Interestingly, no significant functional connectivity of LC with striatal regions was found in the PPI analysis.

Tonic and phasic activity modes of LC neurons have been described [Aston-Jones and Bloom, 1981; Aston-Jones and Cohen, 2005]. The LC-NA tonic signal regulates transitions between specific behavioral states, such as sleep or focused attention. The pattern of tonic activity follows the classical Yerkes-Dodson relationship between arousal and performance [Aston-Jones and Cohen, 2005].

Phasic LC activity might provide a temporal attentional filter, which selectively facilitates behavioral responses to task-relevant features and optimizes task-appropriate behavior [Aston-Jones and Cohen, 2005]. Prefrontal and anterior cingulate inputs were assumed to enable the transition between different tonic levels as well as to trigger the LC phasic response [Clayton et al., 2004; Corbetta, et al., 2008]. Both excitatory as well as inhibitory influences from the PFC on LC have been described [Sara and Herve-Minvielle, 1995]. With respect to this interaction, Sara and Bouret [2012] stated that the firing of frontal neurons due to an increased cognitive demand "wake up" the LC, which in turn facilitates cortical processing. Thus, LC functioning is supposed to mediate activity and functional integration of the cognitive control network, including the frontal cortex, thalamus and posterior cortical regions, and to modulate dynamic plasticity of cognitive brain systems [Coull et al., 1999].

As described above, Corbetta et al. [2008] hypothesized that signals from the LC influence adaptive state shifts between the ventral and dorsal fronto-parietal networks. Supporting this theory, Hermans et al. [2011] provided strong evidence that noradrenalin is a key neuromodulator of the acute stress response, which is associated with state shifts in specific attentional control related networks.

In agreement with the theory proposed by Corbetta et al. [2008], we observed in the PPI analysis a significant functional connectivity of the LC as modulated by the cognitive control demand with the dorsal fronto-cingulo-parietal network. However, the precise temporal pattern in terms of a causal relationship between LC activity and the reorganization in the task-related dorsal and salience-related ventral fronto-parietal networks needs to be investigated in further studies using superior temporal and spatial resolution.

Summarizing previous results and our findings, we assume that the phasic LC signals facilitate cognitive conflict resolution and optimize behavioral responses to incongruent Stroop items by activating a specific task-related brain network and further by amplifying task-relevant features, as reflected by strong functional connectivity to the occipital, pre-/motor and superior parietal cortices.

Interestingly, whereas a strong linear decrease of BOLD activation was detected in the fronto-cingulo-striatal network as well as in the parietal and occipital regions, we did not observe such a linear decrease in activation regarding the LC. This finding indicates that despite the diminished need of cognitive control over time as reflected in a significant linear decline of the RTs in the incongruent Stroop task condition, the activation of the LC did not significantly change over the course of the experiment.

The precise location of the LC is an important issue in this study. Previous studies have described seven NA cell groups (A1–A7) in rodents and primates [Dahlstroem and Fuxe, 1964; Schofield and Everitt, 1981], which are situated at the pontine and medullary tegmental level. Nieuwenhuys [1985] suggested that the cell groups A4 and A6 form the LC complex, whereas other authors suggested the cell groups A4–A7 [Pearson et al., 1983]. The LC proper was described as a bilateral, "tube-like," pigmented nucleus [Fernandes et al., 2012; German et al., 1988]. It begins rostrally in the caudolateral part of the mesencephalic central gray, at the level of the inferior colliculus (A6), and extends caudally to a position in the lateral wall of the fourth ventricle (A4) [German, et al., 1988]. The LC measures ~16 mm long by 2 mm wide by 1.8 mm deep at the central zone [Fernandes, et al., 2012; German, et al., 1988]. The NA cell group A5, which is termed as nucleus subcoeruleus, extends ventrolaterally from the caudal pole of the LC (A4) [Bogerts, 1981]. The cell group A7 is situated in the rostral pons. This cell group connects the rostral part of the LC with the caudal poles of the dopaminergic SN and the VTA [Bogerts, 1981]. The relative ventral and rostral LC activation during the contrast incongruent vs. congruent condition most likely represents the A7 nucleus, whereas the more caudal position of the LC in the regression analysis might represent the nucleus subcoeruleus (A5 cell group).

Furthermore, LC coordinates in this study are in line with reported coordinates of previous fMRI studies. Minzenberg et al. [2008] used modafinil in healthy humans, a pharmacological agent, which increases synaptic NE and DA levels by inhibiting NA and DA transporters. Thereby the authors modulated the activation level of the LC while performing a cognitive control task, similarly to the Stroop task. Modafanil administration was associated with decreased task-independent, tonic LC activity, increased task-related LC and PFC activity, and enhanced LC-PFC functional connectivity.

Bearing in mind the isotropic resolution of 3.4 mm^3 and a smoothing kernel of 8 mm used in the study by Minzenberg et al. [2008], the reported MNI coordinates of the LC based on the contrast modafinil challenge vs. placebo were coherent with the present position of LC in the incongruent vs. congruent contrast. In addition, Murphy et al. [2014] showed in a study combining pupillometry and fMRI a significant relationship between activation in the LC and pupil diameter in the resting state condition as well as during performance of an oddball task. Interestingly, the MNI coordinates of the LC during the oddball task overlapped with LC coordinates detected in the regression analysis of this study.

Using tract-tracing experiments in rats, Chandler et al. [2014] recently demonstrated that opposed to the

traditional view the LC exhibits functional differences depending on the terminal fields of LC neurons. The authors observed that LC neurons projecting to PFC in rats are more excitable and display higher spontaneous firing frequencies than those projecting to the motor cortex (2014). Furthermore, this observation implies a potentially differential NA modulation of PFC-dependent executive functions and behavioral outcomes, depending on cortical/subcortical motor circuitry. This finding can potentially explain the slight differences in the LC activation along the rostrocaudal axis found in this study. Comparing the incongruent vs. congruent condition, we observed BOLD signal differences in a more rostral part of the LC complex (corresponding to A7 cell group), whereas the cluster of significant correlation between LC BOLD signal and reaction time differences between incongruent and congruent condition was situated more ventrally in the subcoeruleus and in the A6. Thus, this observation might be consistent with the notion that given the anatomical heterogeneity of the LC complex in the brainstem and therefore potential varying cortical/subcortical connectivity, different parts of the LC are specifically contributing to distinct subcomponents of cognitive control processes, such as cognitive conflict monitoring/resolution mainly based on the fronto-cingulate circuitry and inhibition of prepotent motor responses (due to the motor version of the employed Stroop task in this study) mainly based on the SMA/premotor/motor cortices. However, this interpretation warrants further studies to elucidate the contribution of specific LC nuclei to different cognitive control processes in more detail.

We did not observe a significant functional connectivity between the LC, SN/VTA, and striatal regions. Nevertheless, NA modulation of cognitive functioning is likely to depend on the cooperation of a distributed network of brain regions, acting together in a functionally integrated way, as observed in the overlapping functional connectivity between VTA/SN and LC with dACC, SMA, and parietal regions. Ventura et al. [2003] analyzed the effects of medial PFC noradrenaline depletion in mice and showed an absence of amphetamine-induced conditioned place preference as well as a reduced amphetamine-induced mesoaccumbens DA release. In different psychiatric disorders such as schizophrenia, major depression, attention-deficit/hyperactivity disorder (ADHD) or obsessive-compulsive disorder, poor inhibition-related processes were assumed to be associated with abnormal monoaminergic neurotransmission [Arnsten and Rubia, 2012; Nigg, 2001]. For example, methylphenidate (MPH) and atomoxetine (ATX) are often administered to treat ADHD in children or adolescents [Hazell et al., 2011]. MPH blocks DA transporters (DAT) in the striatum and noradrenaline transporters mainly in thalamic and frontal regions, enhancing thereby DA and NA neurotransmission [Hannestad et al., 2010; Volkow et al., 1998]. Moeller et al. [2014] found that the consumption of MPH enhanced the Stroop task performance and modulated BOLD activation in prefrontal cortical areas. ATX also affects both catecholamines in the PFC and NA in the thalamus, LC, cerebellum, and striatum [Bymaster et al., 2002; Gallezot et al., 2011]. Chou et al. [2015] studied the effects of 12-weeks treatment with ATX and MPH in children with ADHD and found improved inhibitory control. In an fMRI-study of Cubillo et al. [2014], the authors found that ATX up-regulated and normalized right DLPFC underactivation in children suffering from ADHD during a working memory task, while MPH up-regulated left VLPFC activation. Furthermore, MPH was found to significantly normalize the fronto-striatal underactivation in ADHD patients during interference inhibition [Rubia et al., 2011]. Thus, ATX and MPH were suggested to enhance fronto-striatal activation leading to increased inhibitory control in patients with ADHD due to an increase of NA and dopaminergic neurotransmission. In addition, similar effects of ATX on response inhibition and fronto-striatal activation as well as connectivity were detected in patients with Parkinson's Disease [Ye et al., 2015], emphasizing the mutual role of NA- and DA-systems in regulating response inhibition. Our results of LC and VTA/SN activation as well as functional connectivity findings are well in line with these studies indicating a crucial role of both DA and NA neurotransmitter systems in inhibitory control.

Thus, the findings of this study may provide an interesting approach to investigate the putatively abnormal interaction between midbrain/brainstem nuclei and the cortical regions in different neurological and psychiatric disorders in the future.

A number of limitations in our study should be noted. The nuclei within brainstem and midbrain are small compared with the cortical regions activated during cognitive control, and are more susceptible to signal distortion and artifacts arising from local tissue interfaces and physiological noise. Therefore, further studies with increased spatial resolution are required to support our findings. In addition, the current study lacks additional behavioral measurements (e.g., pupillometry) which have recently been shown to specifically track LC activity [Joshi et al., 2016]. Moreover, to more precisely define the anatomical position of the LC, an additional acquisition of a high resolution brainstem structural image may be necessary in future studies. For example, using a T1-weighted Turbo Spin Echo (T1-TSE) imaging protocol by Sasaki et al. [2006] and Keren et al. [2009] successfully visualized the LC in the 3T scanner. The T1-TSE sequence allows identification of LC by means of a neuromelanin-sensitive contrast. Recently, Keren et al. [2015] provided a histological validation that the neuromelanin-related LC contrast in the T1 images corresponded to the shape and distribution of LC in post-mortem tissue samples. However, in contrast to structural imaging, functional imaging relies on blood-oxygen-level-dependent (BOLD) contrast as the basic principle for detecting neuronal activation. The spatial accuracy and

extension of the activation maps in specific brain regions, especially in the brainstem are heavily dependent on the vascular effect, which may introduce incertitude with respect to real neuronal activation site. This might be one reason for the slight difference in the LC position between our (more ventrally located) as well as previous functional studies and the structural neuromelanin-sensitive T1-TSE MRI studies. Thus, to gain more confidence in the definite location of small brain stem nuclei, a combination of sophisticated structural and functional imaging techniques and simultaneous behavioral measurements is needed in the future.

In summary, our study represents the first direct demonstration of the functional integration of the noradrenaline producing LC and dopaminergic nuclei SN/VTA within the cognitive control network in the human brain. Since catecholaminergic neurotransmission is essential to neocortical and subcortical functions, and represents an important target for pharmacotherapy, our novel findings contribute to a comprehensive understanding of the functional organization of the human brain and, in particular, to the broader understanding of the importance of the DA as well as NA systems for executive functions with potentially far-reaching implications for pathophysiological conditions and psychopharmacology.

REFERENCES

Alexander GE, Crutcher MD (1990): Functional architecture of basal ganglia circuits: neural substrates of parallel processing. Trends Neurosci 13:266–271.

Alexander GE, DeLong MR, Strick PL (1986): Parallel organization of functionally segregated circuits linking basal ganglia and cortex. Annu Rev Neurosci 9:357–381.

Amalric M, Koob GF (1993): Functionally selective neurochemical afferents and efferents of the mesocorticolimbic and nigrostriatal dopamine system. Prog Brain Res 99:209–226.

Arnsten AF, Rubia K (2012): Neurobiological circuits regulating attention, cognitive control, motivation, and emotion: disruptions in neurodevelopmental psychiatric disorders. J Am Acad Child Adolesc Psychiatry 51:356–367.

Ashburner J (2007): A fast diffeomorphic image registration algorithm. Neuroimage 38:95–113.

Aston-Jones G, Bloom FE (1981): Activity of norepinephrine-containing locus coeruleus neurons in behaving rats anticipates fluctuations in the sleep-waking cycle. J Neurosci 1:876–886.

Aston-Jones G, Cohen JD (2005): An integrative theory of locus coeruleus-norepinephrine function: adaptive gain and optimal performance. Annu Rev Neurosci 28:403–450.

Beg MF, Miller MI, Trouve A, Younes L (2005): Computing large deformation metric mappings via geodesic flows of diffeomorphisms. Int J Comput Vis 61:139–157.

Bogerts B (1981): A Brain-Stem Atlas of Catecholaminergic Neurons in Man, Using Melanin as a Natural Marker. J Comp Neurol 197:63–80.

Bolla K, Ernst M, Kiehl K, Mouratidis M, Eldreth D, Contoreggi C, Matochik J, Kurian V, Cadet J, Kimes A, Funderburk F, London E (2004): Prefrontal cortical dysfunction in abstinent cocaine abusers. J Neuropsychiatry Clin Neurosci 16:456–464.

Botvinick MM, Braver TS, Barch DM, Carter CS, Cohen JD (2001): Conflict monitoring and cognitive control. Psychol Rev 108: 624–652.

Bouret S, Sara SJ (2005): Network reset: A simplified overarching theory of locus coeruleus noradrenaline function. Trends Neurosci 28:574–582.

Briggs GG, Nebes RD (1975): Patterns of hand preference in a student population. Cortex 11:230–238.

Bymaster FP, Katner JS, Nelson DL, Hemrick-Luecke SK, Threlkeld PG, Heiligenstein JH, Morin SM, Gehlert DR, Perry KW (2002): Atomoxetine increases extracellular levels of norepinephrine and dopamine in prefrontal cortex of rat: A potential mechanism for efficacy in attention deficit/hyperactivity disorder. Neuropsychopharmacology 27:699–711.

Chandler DJ, Gao WJ, Waterhouse BD (2014): Heterogeneous organization of the locus coeruleus projections to prefrontal and motor cortices. Proc Natl Acad Sci U S A 111:6816–6821.

Chou TL, Chia S, Shang CY, Gau SS (2015): Differential therapeutic effects of 12-week treatment of atomoxetine and methylphenidate on drug-naive children with attention deficit/hyperactivity disorder: A counting Stroop functional MRI study. Eur Neuropsychopharmacol 25:2300–2310.

Clayton EC, Rajkowski J, Cohen JD, Aston-Jones G (2004): Phasic activation of monkey locus ceruleus neurons by simple decisions in a forced-choice task. J Neurosci 24:9914–9920.

Corbetta M, Patel G, Shulman GL (2008): The reorienting system of the human brain: From environment to theory of mind. Neuron 58:306–324.

Coull JT, Buchel C, Friston KJ, Frith CD (1999): Noradrenergically mediated plasticity in a human attentional neuronal network. Neuroimage 10:705–715.

Cubillo A, Smith AB, Barrett N, Giampietro V, Brammer M, Simmons A, Rubia K (2014): Drug-specific laterality effects on frontal lobe activation of atomoxetine and methylphenidate in attention deficit hyperactivity disorder boys during working memory. Psychol Med 44:633–646.

Dahlstroem A, Fuxe K (1964): Evidence for the existence of monoamine-containing neurons in the central nervous system. I. Demonstration of Monoamines in the Cell Bodies of Brain Stem Neurons. Acta Physiol Scand Suppl 232(SUPPL):1–55.

Devauges V, Sara SJ (1990): Activation of the noradrenergic system facilitates an attentional shift in the rat. Behav Brain Res 39:19–28.

Diedrichsen J (2006): A spatially unbiased atlas template of the human cerebellum. Neuroimage 33:127–138.

Fernandes P, Regala J, Correia F, Goncalves-Ferreira AJ (2012): The human locus coeruleus 3-D stereotactic anatomy. SRA 34: 879–885.

Foote SL, Bloom FE, Aston-Jones G (1983): Nucleus locus ceruleus: New evidence of anatomical and physiological specificity. Physiol Rev 63:844–914.

Fuxe K, Hamberger B, Hokfelt T (1968): Distribution of noradrenaline nerve terminals in cortical areas of the rat. Brain Res 8: 125–131.

Gallezot JD, Weinzimmer D, Nabulsi N, Lin SF, Fowles K, Sandiego C, McCarthy TJ, Maguire RP, Carson RE, Ding YS (2011): Evaluation of [(11)C]MRB for assessment of occupancy of norepinephrine transporters: Studies with atomoxetine in non-human primates. Neuroimage 56:268–279.

German DC, Walker BS, Manaye K, Smith WK, Woodward DJ, North AJ (1988): The human locus coeruleus: Computer reconstruction of cellular distribution. J Neurosci 8:1776–1788.

Grahn JA, Parkinson JA, Owen AM (2008): The cognitive functions of the caudate nucleus. Prog Neurobiol 86:141–155.

Haber SN (2003): The primate basal ganglia: parallel and integrative networks. J Chem Neuroanat 26:317–330.

Haber SN, Fudge JL, McFarland NR (2000): Striatonigrostriatal pathways in primates form an ascending spiral from the shell to the dorsolateral striatum. J Neurosci 20:2369–2382.

Hannestad J, Gallezot JD, Planeta-Wilson B, Lin SF, Williams WA, van Dyck CH, Malison RT, Carson RE, Ding YS (2010): Clinically relevant doses of methylphenidate significantly occupy norepinephrine transporters in humans in vivo. Biol Psychiatry 68:854–860.

Hazell PL, Kohn MR, Dickson R, Walton RJ, Granger RE, Wyk GW (2011): Core ADHD symptom improvement with atomoxetine versus methylphenidate: A direct comparison meta-analysis. J Attention Disord 15:674–683.

Hermans EJ, van Marle HJ, Ossewaarde L, Henckens MJ, Qin S, van Kesteren MT, Schoots VC, Cousijn H, Rijpkema M, Oostenveld R, Fernandez G (2011): Stress-related noradrenergic activity prompts large-scale neural network reconfiguration. Science (New York) 334:1151–1153.

Ikemoto S (2007): Dopamine reward circuitry: Two projection systems from the ventral midbrain to the nucleus accumbens-olfactory tubercle complex. Brain Res Rev 56:27–78.

Joshi S, Li Y, Kalwani RM, Gold JI (2016): Relationships between Pupil Diameter and Neuronal Activity in the Locus Coeruleus, Colliculi, and Cingulate Cortex. Neuron 89:221–234.

Keren NI, Lozar CT, Harris KC, Morgan PS, Eckert MA (2009): In vivo mapping of the human locus coeruleus. Neuroimage 47: 1261–1267.

Keren NI, Taheri S, Vazey EM, Morgan PS, Granholm AC, Aston-Jones GS, Eckert MA (2015): Histologic validation of locus coeruleus MRI contrast in post-mortem tissue. Neuroimage 113:235–245.

Koch K, Wagner G, von Consbruch K, Nenadic I, Schultz C, Ehle C, Reichenbach J, Sauer H, Schlosser R (2006): Temporal changes in neural activation during practice of information retrieval from short-term memory: An fMRI study. Brain Res 1107:140–150.

Kunishio K, Haber SN (1994): Primate cingulostriatal projection: limbic striatal versus sensorimotor striatal input. J Comp Neurol 350:337–356.

Mair RD, Zhang Y, Bailey KR, Toupin MM, Mair RG (2005): Effects of clonidine in the locus coeruleus on prefrontal- and hippocampal-dependent measures of attention and memory in the rat. Psychopharmacology (Berl) 181:280–288.

Mannella F, Gurney K, Baldassarre G (2013): The nucleus accumbens as a nexus between values and goals in goal-directed behavior: A review and a new hypothesis. Front Behav Neurosci 7:135.

Mansouri FA, Tanaka K, Buckley MJ (2009): Conflict-induced behavioural adjustment: A clue to the executive functions of the prefrontal cortex. Nat Rev Neurosci 10:141–152.

Milham MP, Banich MT, Claus ED, Cohen NJ (2003): Practice-related effects demonstrate complementary roles of anterior cingulate and prefrontal cortices in attentional control. Neuroimage 18:483–493.

Miller EK, Cohen JD (2001): An integrative theory of prefrontal cortex function. Annu Rev Neurosci 24:167–202.

Minzenberg MJ, Watrous AJ, Yoon JH, Ursu S, Carter CS (2008): Modanfinil Shifts Human Locus Coeruleus to Low-Tonic, High-Phasic Activity During Functional MRI. Science (New York) 322:1700–1702.

Moeller SJ, Honorio J, Tomasi D, Parvaz MA, Woicik PA, Volkow ND, Goldstein RZ (2014): Methylphenidate enhances executive function and optimizes prefrontal function in both health and cocaine addiction. Cerebral Cortex (New York) 24:643–653.

Murphy PR, O'Connell RG, O'Sullivan M, Robertson IH, Balsters JH (2014): Pupil diameter covaries with BOLD activity in human locus coeruleus. Hum Brain Mapp 35:4140–4154.

Naidich TP, Duvernoy HM, Delman BN, Sorensen AG, Kollias SS, Haacke EM (2009): Duvornoy's Atlas of the Human Brain Stem and Cerebellum. Wien: Springer.

Nieuwenhuys R. (1985): Chemoarchitecture of the brain. Berlin: Springer.

Nigg JT (2001): Is ADHD a disinhibitory disorder? Psychol Bull 127:571–598.

O'Doherty JP, Dayan P, Friston K, Critchley H, Dolan RJ (2003): Temporal difference models and reward-related learning in the human brain. Neuron 38:329–337.

O'Doherty JP, Buchanan TW, Seymour B, Dolan RJ (2006): Predictive neural coding of reward preference involves dissociable responses in human ventral midbrain and ventral striatum. Neuron 49:157–166.

Parent A (1990): Extrinsic connections of the basal ganglia. Trends Neurosci 13:254–258.

Pearson J, Goldstein M, Markey K, Brandeis L (1983): Human Brain-Stem Catecholamine Neuronal Anatomy as Indicated by Immunocytochemistry with Antibodies to Tyrosine-Hydroxylase. Neuroscience 8:3–32.

Raizada RD, Poldrack RA (2008): Challenge-driven attention: Interacting frontal and brainstem systems. Front Human Neurosci 1:3.

Rubia K, Halari R, Cubillo A, Smith AB, Mohammad AM, Brammer M, Taylor E (2011): Methylphenidate normalizes fronto-striatal underactivation during interference inhibition in medication-naive boys with attention-deficit hyperactivity disorder. Neuropsychopharmacology 36:1575–1586.

Salo R, Ursu S, Buonocore MH, Leamon MH, Carter C (2009): Impaired prefrontal cortical function and disrupted adaptive cognitive control in methamphetamine abusers: A functional magnetic resonance imaging study. Biol Psychiatry 65:706–709.

Sara SJ, Bouret S (2012): Orienting and reorienting: the locus coeruleus mediates cognition through arousal. Neuron 76: 130–141.

Sara SJ, Herve-Minvielle A (1995): Inhibitory influence of frontal cortex on locus coeruleus neurons. Proc Natl Acad Sci U S A 92:6032–6036.

Sasaki M, Shibata E, Tohyama K, Takahashi J, Otsuka K, Tsuchiya K, Takahashi S, Ehara S, Terayama Y, Sakai A (2006): Neuromelanin magnetic resonance imaging of locus ceruleus and substantia nigra in Parkinson's disease. Neuroreport 17:1215–1218.

Schofield SPM, Everitt BJ (1981): The organization of catecholamine-containing neurons in the brain of the Rhesus-Monkey (Macaca-Mulatta). J Anat 132:391–418.

Sheehan DV, Lecrubier Y, Sheehan KH, Amorim P, Janavs J, Weiller E, Hergueta T, Baker R, Dunbar GC (1998): The Mini-International Neuropsychiatric Interview (M.I.N.I.): the development and validation of a structured diagnostic psychiatric interview for DSM-IV and ICD-10. J Clin Psychiatry 59:22–33. quiz 34-57.

Stroop JR (1935): Studies of interference in serial verbal reactions. J Exp Psychol 18:643–662.

Tait DS, Brown VJ, Farovik A, Theobald DE, Dalley JW, Robbins TW (2007): Lesions of the dorsal noradrenergic bundle

impair attentional set-shifting in the rat. Eur J Neurosci 25: 3719–3724.

Tomasi D, Volkow ND (2014): Functional connectivity of substantia nigra and ventral tegmental area: Maturation during adolescence and effects of ADHD. Cerebral cortex (New York) 24: 935–944.

Ungerstedt U (1971): Stereotaxic mapping of the monoamine pathways in the rat brain. Acta Physiol Scand Suppl 367:1–48.

Ventura R, Cabib S, Alcaro A, Orsini C, Puglisi-Allegra S (2003): Norepinephrine in the prefrontal cortex is critical for amphetamine-induced reward and mesoaccumbens dopamine release. J Neurosci 23:1879–1885.

Volkow ND, Wang GJ, Fowler JS, Gatley SJ, Logan J, Ding YS, Hitzemann R, Pappas N (1998): Dopamine transporter occupancies in the human brain induced by therapeutic doses of oral methylphenidate. Am J Psychiatry 155:1325–1331.

Wagner G, De la Cruz F, Schachtzabel C, Gullmar D, Schultz CC, Schlosser RG, Bär KJ, Koch K (2015): Structural and functional dysconnectivity of the fronto-thalamic system in schizophrenia: A DCM-DTI study. Cortex 66:35–45.

Woo CW, Krishnan A, Wager TD (2014): Cluster-extent based thresholding in fMRI analyses: pitfalls and recommendations. Neuroimage 91:412–419.

Ye Z, Altena E, Nombela C, Housden CR, Maxwell H, Rittman T, Huddleston C, Rae CL, Regenthal R, Sahakian BJ, Barker RA, Robbins TW, Rowe JB (2015): Improving Response Inhibition in Parkinson's Disease with Atomoxetine. Biol Psychiatry 77: 740–748.